J Mol Model (2014) 20:2105
DOI 10.1007/s00894-014-2105-z

ORIGINAL PAPER

Structure and electronic properties of (+)-catechin: aqueous solvent effects

Erika N. Bentz · Alicia B. Pomilio · Rosana M. Lobayan

Received: 4 August 2013 / Accepted: 9 December 2013 / Published online: 14 February 2014

Abstract We report a study of the structure of (+)-catechin, which belongs to the family of the flavan-3-ols—one of the five most widely distributed phenolic groups. The biological activities and pharmaceutical utility of these compounds are related to antioxidant activity due to their ability to scavenge free radicals. A breakthrough in the study of the conformational space of this compound, so far absent in the literature, is presented herein. A detailed analysis of the electronic distribution, charge delocalization effects, and stereoelectronic effects is presented following application of the theory of atoms in molecules (AIM) and natural bond orbital analysis. The stability order, and the effects of electron delocalization in the structures were analyzed in depth. The molecular electrostatic potential (MEP) was also obtained, assessing changes in the electronic distribution in aqueous solution, the effects of the solvent on the intrinsic electronic properties, and molecular geometry. The effect of the aqueous solvent on MEP was also quantified, and rationalized by charge delocalization mechanisms, relating them to structural changes and topological properties of the electronic charge density. To further analyze the effects of the aqueous solvent, as well as investigating the molecular and structural properties of these compounds in a biological environment, the polarizabilities for all conformers characterized were also calculated. All results were interpreted on the basis of our accumulated knowledge on (4α→6", 2α→*O*→1")-phenylflavans in previous reports, thus enriching and deepening the analysis of both types of structure.

Keywords (+)-Catechin · Antioxidants · Density functional theory · Aqueous solvent effect · PCM model · Atoms in molecules · Natural bond orbital analysis · Molecular polarizability

Electronic supplementary material The online version of this article (doi:10.1007/s00894-014-2105-z) contains supplementary material, which is available to authorized users.

E. N. Bentz · R. M. Lobayan
Instituto de Investigaciones Científicas, Universidad de la Cuenca del Plata, Facultad de Ingeniería, Lavalle 50, 3400 Corrientes, Argentina

A. B. Pomilio
Instituto de Bioquímica y Medicina Molecular [IBIMOL (ex PRALIB), UBA-CONICET], Facultad de Farmacia y Bioquímica, Universidad de Buenos Aires, Junín 956, C1113AAD Buenos Aires, Argentina

R. M. Lobayan (✉)
Departamento de Física, Facultad de Ciencias Exactas y Naturales y Agrimensura, Universidad Nacional del Nordeste, Avda. Libertad 5300, 3400 Corrientes, Argentina
e-mail: rmlb@exa.unne.edu.ar

Introduction

Structures known as flavonoids comprise a wide range of phytocompounds occurring in fruits, vegetables, roots, and flowers. Their structures are based on a flavan moiety, and are classified according to the degree of saturation of the pyran ring (ring C), and further substitution on this ring.

Flavonoids consist of a benzene ring (A) fused to a six-membered ring (C), which, in the case of the flavonols and flavones, is a γ-pyran that contains a phenyl group (B) in position 2 (C-2), and a carbonyl group at C-4. Isoflavonoids have the phenyl group at C-3. Catechins lack both the carbonyl at C-4 and the 2,3-double bond (Fig. 1).

The structural diversity of flavonoids results in a variety of bioactivities, including anti-inflammatory, antiherpetic, antiallergic, antibacterial, antimutagenic, anti-thrombosis, antiviral, antioxidant, anticarcinogenic, and vasodilator activities [1–5]. Flavonoids are also responsible for the color of the vegetables and fruits, due to anthocyanins, and are associated with protection against UV and microbial invasion [6, 7]. These effects have been attributed mainly to antioxidant

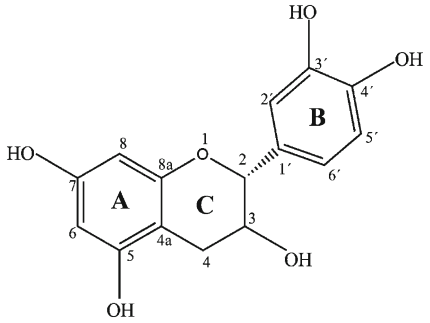

Fig. 1 Structure of (+)-catechin. The numbering used for the analysis is shown

activity, which has many applications in the pharmaceutical, food and agriculture industries.

The role of flavonoids as antioxidants has been the subject of intense research, both theoretical and experimental, in recent years [8–11].

The biological activities and pharmaceutical utilities of these compounds are related to the antioxidant activity due to their ability to scavenge free radicals. Free radicals are known to damage biomolecules such as lipids, amino acids, proteins, carbohydrates, and nucleic acids by oxidative processes, resulting in numerous diseases. Oxidative stress is a phenomenon associated with the imbalance between antioxidants and free radical generation [12].

The molecular basis of the antioxidant properties of flavonoids remains unclear to date due to the limited knowledge both of their intrinsic properties, and of the relationship of these properties to the structure, as well as the variability of experimental data generated. Some authors have proposed that the antioxidant mechanism of flavonoids is based on processes related to direct and indirect transfer of the hydrogen atom to free radicals. Antioxidant activity has been correlated to molecular structure, more precisely to the presence and number of OH groups, and with the effects of conjugation and electron resonance [13].

In this work, we studied the structure of (+)-catechin, which belongs to the flavan-3-ols, i.e., one of the five largest phenolic groups distributed widely in nature. (+)-Catechin is found mainly in white and red wine, and especially in green and black tea, together with epicatechin (EC), epigallocatechin (EGC), epicatechin gallate, and epigallocatechin gallate (EGCG), which are responsible for anticarcinogenic activity [3]. Hydroxylation occurs in positions 3′ and 4′ of the catechol ring (ring B), and C-5 and C-7 of the resorcinol ring (ring A) as shown in Fig. 1.

Investigations on this flavonoid have been reported previously [10, 14–16]. Some properties of catechin were studied in gas phase, and calculations of reactivity descriptive parameters were analyzed, also considering the effect of different solvents. In general, reports are based on a single conformer selected by its energy stability. To our knowledge, no study of the conformational space of this compound has been reported in the literature. Moreover, no reports on the stability of the electronic distribution, charge delocalizations effects, and stereoelectronic effects by atoms in molecules (AIM) theory and/or natural bond orbital (NBO) analysis have appeared.

According to the literature, the catechol moiety (ring B) is necessary to enhance the antioxidant activity of most natural antioxidants but, due to knowledge acquired regarding the role played by the resorcinol moiety in similar structures [17–20], we undertook a detailed study aimed at analyzing the effects of both ring B and ring A.

We also aimed to analyze the stability order, providing an in depth description of the effects of electron delocalization operating in these structures.

It is worth mentioning that other authors have reported variations in the structural, thermochemical and magnetic properties in various commercial samples, thus revealing the existence of different conformational mixtures [21]. Indeed, the difficulty in correlating theoretical and experimental data because of conformer mixture occurrence in samples (although very pure) makes it necessary to consider the relative weight of each one. These results highlight the importance of theoretical studies, and the usefulness of progress in our detailed knowledge of conformational space.

Furthermore, although the theoretical results of an isolated molecule are very useful for determining the intrinsic properties of the system free of any kind of interaction, such results can be compared with experimental data in only a few cases, since most assays are performed in solution. Therefore, to be able to make observations on the structural and intrinsic electronic properties and, considering that water is the main component of physiological fluids, in this study we reoptimized minimum energy structures obtained in vacuum, taking into account the effect of aqueous solvent, simulated by the polarizable continuum model (PCM) [22].

Changes in the electronic distribution of (+)-catechin in aqueous solution were evaluated, and the effects of the solvent on the intrinsic electronic properties and molecular geometry were analyzed. Moreover, the molecular electrostatic potential (MEP) was obtained, and analyzed in depth. The effect of the aqueous solvent on MEPs was also quantified, and rationalized by charge delocalization mechanisms, thus relating MEPs modifications with structural changes, and topological properties.

To further analyze the effects of the aqueous solvent, and the molecular and structural properties in a biological environment, polarizabilities were also calculated.

All results were interpreted in terms of the accumulated knowledge derived from our previous reports on (4α→6″, 2α→*O*→1″)-phenylflavans [19], which allowed us to enrich and deepen the analysis of both types of structure.

Methods

All computational study was performed by the density functional theory (DFT), as implemented by the Gaussian 03 package [23]. An analysis of the conformational space using the Becke 3-parameter hybrid functional and the Lee-Yang-Parr correlation functional was performed. This combination gave rise to the method known as B3LYP [24, 25]. The 6-31G (d,p) basis set was used for all atoms. The reliability of the selected calculation level has been reported previously [11, 26, 27].

The profiles of the potential energy surfaces were obtained by performing a rigid scan rotating ring B (setting the dihedral angle (τ), C3–C2–C1′–C2 ′) around the C2–C1′ bond in steps of 30°.

Then, taking the minimum energy conformations and the corresponding transition states, reoptimizations were carried out with totally relaxed geometries at the same level of theory. Harmonic vibrational frequencies were calculated, and analyzed at the same level to confirm the presence of true minimum energy structures or transition states, as well as to perform thermodynamic corrections that are included in all electronic energies reported.

Chemical bonds were studied and characterized by AIM theory [28], including NBO analysis [29]. Topological analysis and the evaluation of local properties were performed with PROAIM software [30] using the wave functions calculated at B3LYP level, and with the improved 6-311++ G(d,p) base implemented in the G03 program. NBO analysis was performed at this level.

The lowest energy conformers obtained and selected from the analysis in gas phase were further reoptimized considering the effect of solvent by PCM [22] at the same level of theory [B3LYP/6-31G(d,p)]. The PCM approach considers that the molecule under study is inside a cavity embedded in a polarizable dielectric, allowing solvent modeling by choosing the proper dielectric constant without the explicit inclusion of solvent molecules. The polarizable dielectric medium was characterized by a dielectric constant, ε=78.35 for water. The average values of surface area, and cavity volume were 340.201 $Å^2$ and 370.121 $Å^3$, respectively. This model has proven to be a reliable tool for the description of solute-solvent electrostatic interactions.

Moreover, the MEP on the van der Waals surface of each molecule under study was obtained using G03 software, and displayed by Molekel 4.0 software [31].

Results and discussion

Conformational and structural analysis

The study of the conformational space of (+)-catechin (CTQ) was progressed from previous knowledge obtained regarding the most stable conformation of the resorcinol-ring in (4α→6″, 2α→*O*→1″)-phenylflavans [18] by fixing the positions of the hydroxy groups at C-5 and C-7, as shown in Fig. 2. This conformer was called CT-type. This designation referred to syn (cis) and anti (trans) configurations of H–O5 and H–O7 bonds relative to C5–C6 and C6–C7 bonds, respectively, in ring A (resorcinol-type). The average values of the dihedral angles H–O5–C5–C6 and H–O7–C7–C6 were close to 0° (cis) or close to 180° (trans). Then, the effects of free rotation around the C–O bonds of OH substituents on C-5 and C-7 atoms (ring A), C-3′ and C-4′ (ring B), and C-3 (ring C) were analyzed.

The possible arrangements of the OH groups of the catechol ring allowed the classification of conformers into three groups, indicated by a, b, c, Therefore, CTQa_{CT} group, in which the H of the OH group would form an intramolecular hydrogen bond (HB), was linked to C-4′; the CTQb_{CT} group in which the H of the OH group would form an intramolecular HB, was linked to C-3′; and finally, the group known as CTQc_{CT} with an arrangement of the OH groups that would not allow the formation of any intramolecular HB in ring B (Fig. 2).

Groups defined as *a* and *b* were characterized by the hydrogen atom of the OH groups involved in the HB. According to other authors [9], the structures CTQ*a* and CTQ*b* type are referred to as monohydrate-syn, and CTQ*c* type as dihydrate-anti.

The curves obtained by studying the rotation around the C2–C1′ bond in CTQ*a*, CTQ*b* and CTQ*c*, respectively, are shown in the Electronic Supplementary Material (Figs. S1–S3). Optimized coordinates of minima are shown in Supplementary Tables S1a–S1l.

As reported for (4α→6″, 2α→*O*→1″)-phenylflavans substituted with R′ = H and R = H,OH, and OCH_3 [17, 18], our results showed that the free rotation around C-2–C-1′ led to two types of minima called Z1 and Z2 for each group. We have previously reported for (4α→6″, 2α→*O*→1″)-phenylflavans that Z1-type conformers had the lowest energy, and were characterized by a C3–C2–C1′–C6′ dihedral angle of 88.2°. The same angle for Z2-type isomers accounted for about 0.0°. The angles between the bonds that defined rings C and E, and their respective lengths were quite similar for both conformers; and although the C3–C2–C1′ angle differed by ca. 4.0° for both conformers, Z2 was considered as a rotamer of Z1 [17, 18]. As mentioned above, it is interesting to note that, in the gas phase, similar results were observed for CTQ, as Z1 and Z2 type rotamers were also defined. In this case, the average values for the C1′–C2–C3–C6′ dihedral angle were 85.5 ° and 1.5°, respectively. The C1–C2–C3′ angle also differed by about 4.0° for both conformers. No reference has been found in the literature concerning CTQ conformers of Z2-type.

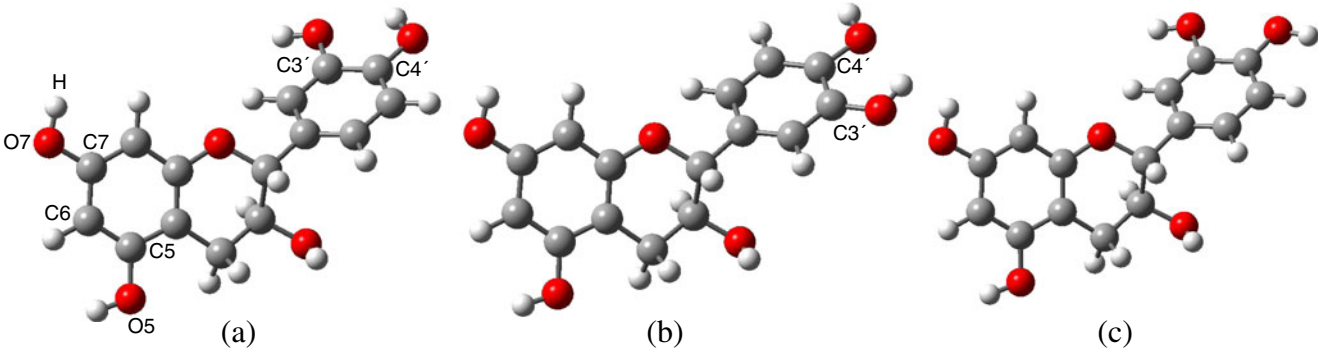

Fig. 2 Structures optimized at B3LYP/6-31G(d,p) level of the most stable conformers for **a** CTQa_{CT}, **b** CTQb_{CT} and **c** CTQc_{CT}

According to the level of calculation, the energy barriers that related Z1 with Z2 structures were lower than 2 kcal mol^{-1}, as shown in Figs. S1–S3 (see Supplementary Material). This low value of barrier suggested the coexistence of both species for the CTQa_{CT} molecule at room temperature. The energy difference between Z1 and Z2 conformers led to relative populations, calculated by the Maxwell-Boltzmann distribution at 298.15 K, of about 4 % for Z2, while for Z1 relative populations varied between 15 % and 35 % (Table 1).

The most stable conformers for each group, and those that show the largest relative population were of the Z1 type, with a τ angle close to 90°, as shown in Table 1. From these, the most stable structure was the so-called CTQ$a1_{CT}$.

The energy difference between the structures of groups *a* and *b* with respect to *c*, and the tiny population of the latter, meant that they were not considered in the deeper study of electronic distribution, as performed below. Furthermore, these results seemed to indicate the stabilizing influence of the intramolecular hydrogen bridge (PH) on the catechol ring. Detailed analysis of such interactions, and changes arising from the inclusion of an aqueous solvent will be discussed below (see Intramolecular hydrogen bridge-type interactions on the catechol ring).

The ± 30° rotation of the angle (τ) around the minimum, in both species (CTQa_{CT} and CTQb_{CT}) led to two transition states (TS), TS2 and TS3 associated with the Z2 rotamer, and two TS (TS1 and TS4) associated with the Z1 rotamer (Figs. S1–S3).

Effect of aqueous solvent on conformational and structural analysis

Including the aqueous solvent by PCM model modified the conformational space. Indeed, the reoptimization of the minimum energy structures found in vacuum always led to Z1 rotamers, which can be explained on the basis of the high instability of Z2 rotamers in vacuum. Therefore, the conformational space was reduced to two conformers for each group

Table 1 Energy calculated at B3LYP/6-31G (d,p) theory level corrected by zero point energy (ZPE), and characteristic τ dihedral angle, for different minimum energy conformers obtained for CTQa_{CT}, CTQb_{CT} and CTQc_{CT} in the gas phase

Conformer	Rotamer	τ angle	Energy (kcal mol^{-1})	ΔE [a] (kcal mol^{-1})	ΔE [b] (kcal mol^{-1})	Relative population [c]
CTQ*a1*	Z1	82.73	−647,025.9689	0.00	0.00	35.09
CTQ*a3*	Z2	176.02	−647,024.2614	1.71	1.71	1.96
CTQ*a2*	Z1	272.52	−647,025.4870	0.48	0.48	15.55
CTQ*a4*	Z2	359.81	−647,024.6586	1.31	1.31	3.84
CTQ*b1*	Z1	84.92	−647,025.6576	0.31	0.00	20.74
CTQ*b3*	Z2	185.84	−647,023.9533	2.02	1.70	1.17
CTQ*b2*	Z1	276.03	−647,025.6288	0.34	0.03	19.76
CTQ*b4*	Z2	357.98	−647,024.2225	1.75	1.44	1.84
CTQ*c1*	Z1	83.64	−647,021.7915	4.18	0.00	0.03
CTQ*c3*	Z2	176.89	−647,020.2943	5.67	1.50	0.00
CTQ*c2*	Z1	270.20	−647,021.4000	4.57	0.39	0.02
CTQ*c4*	Z2	348.21	−647,020.3577	5.61	1.43	0.00

[a] Energy difference relative to the most stable conformer

[b] Energy difference relative to the most stable conformer in each group

[c] Relative Population percentage calculated by Boltzmann, expressed in %

(CTQ$a1_{CT}$, CTQ$a2_{CT}$, CTQ$b1_{CT}$, CTQ$b2_{CT}$, CTQ$c1_{CT}$ and Q$c2_{CT}$) (Fig. 3).

As expected, all structures were more stable in solution than in gas phase, and on average the energy difference for the structures in aqueous solvent and in vacuum was 14.0 kcal mol^{-1}, as shown in Table 2. The analysis showed that the most stable structure was CTQ*b*, and the relative energies with respect to the other conformers were reduced in solution. For (4α→6″,2α→O→1″)-phenylflavan substituted with R = OH, the energy difference for the structures in aqueous solvent and in vacuum was 22.0 kcal mol^{-1} [19]. These results indicated the lesser stabilization in solution of CTQ with respect to the (4α→6″,2α→O→1″)-phenylflavan substituted with R = OH.

Structural parameters of the structures optimized in solution showed small changes with respect to the values in vacuum (see Table S2 in Supplementary Material).

The bond lengths of the C–H, C–C and O–H bonds increased in solution (≈ 0.002 Å), while C–O bond lengths usually decreased. The maximum variation occurred in the bond containing the oxygen that was the hydrogen acceptor in HB, which decreased by 0.006 Å. The C–O bond containing the hydrogen donor oxygen in HB increased slightly (0.002 Å). The C–H bonds of ring A showed no variation. The O–H–C–C dihedral angles varied in ring B up to 4.1°, and in ring A only up to 0.6°, so that in both instances the OH bonds were arranged closer to the plane of each ring. Analyzing the behavior of ring A in (4α→6″, 2α→*O*→1″)-phenylflavan substituted with R = OH, a higher variation was found in solution (C–O bonds decreased up to 0.008 Å; lengthening of O–H, C–H, and C–C bonds up to 0.006 Å, 0.002 Å, and 0.020 Å, respectively) [19]. It is interesting to relate the lower degree of bond length shortening in solution for CTQ to the shortening found in (4α→6″, 2α→*O*→1″)-phenylflavan substituted with R = OH, with the lowest stabilization in solution reported for CTQ.

For CTQ, a difference of up to 14.0° in dihedral angles that defined the position of ring B with respect to the A-C conjugated system (C3–C2–C1′–C2′ and C3–C2, C1′–C6′ dihedral angles) was observed. For (4α→6″, 2α→*O*→1″)-phenylflavan substituted with R = OH, variations in these dihedral angles were less than 2.0°. Therefore, it can be concluded that in CTQ, solvent affected mostly the position of ring B relative to the A-C system, and modified the position of the OH groups on this ring, without influencing the resorcinol-type ring.

Energy differences between all possible conformations of the resorcinol ring with respect to the most stable one (CT type conformer) are shown in Table 3. Thus, as already demonstrated for (4α→6″, 2α→*O*→1″)-phenylflavans [18], the CT-type arrangement of the resorcinol ring in CTQ was the lowest energy conformation. Similar results were found in solution. A solvent attenuated energy difference between conformers was also observed.

Topology of the electronic charge density function

From analysis of the topology of the molecular charge density (ρ), relevant information can be extracted about the molecular structure, whose main characteristics are summarized in the curvatures of the molecular charge density at critical points (CPs). AIM theory [28] is based on the analysis of these CPs [32, 33]. At such points, the gradient of the electron density ∇ρ is zero and is characterized by three eigenvalues, λ_i (i=1–3) of the Hessian matrix. The CPs are named and classified as (r, s) according to their rank, r (number of nonzero eigenvalues), and signature, s (algebraic sum of the signs of the three eigenvalues). The various properties evaluated at bond

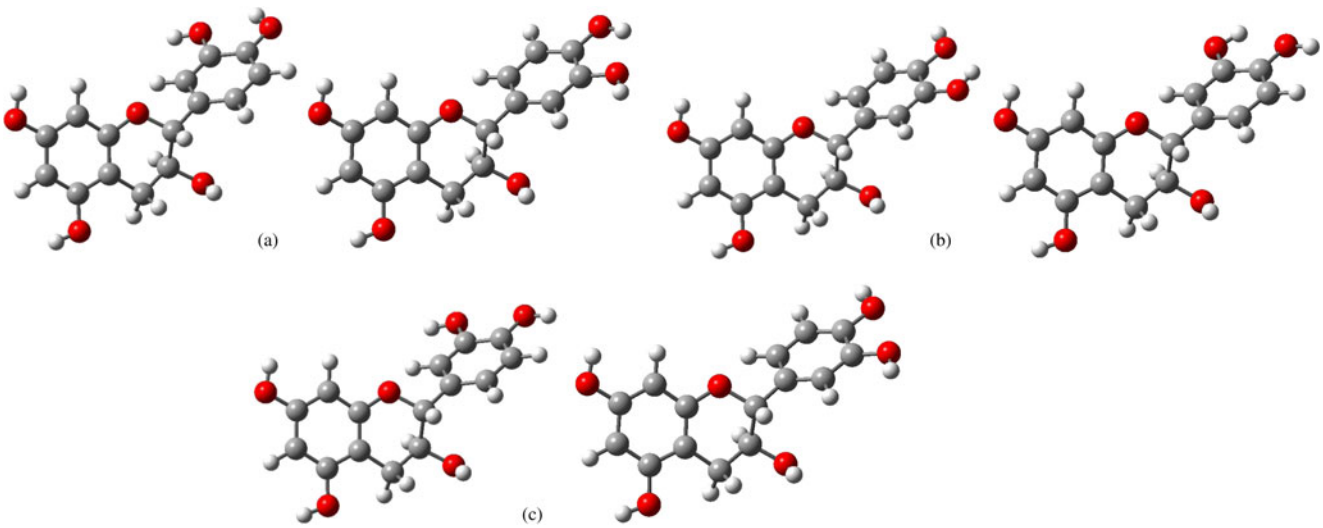

Fig. 3 Structures reoptimized at B3LYP/6-31G(d,p) level in aqueous solution by the polarizable continuum model (PCM) model of the most stable conformers. **a** CTQa_{CT} (CTQ$a1_{CT}$ and CTQ$a2_{CT}$). **b** CTQb_{CT} (CTQb1_{CT} and Q$b2_{CT}$). **c** CTQc_{CT} (CTQ$c1_{CT}$ and CTQ$c2_{CT}$)

Table 2 Energy calculated at the B3LYP/6-31G (d,p) level of theory corrected by ZPE, and characteristic τ dihedral angle, for different conformers of minimum energy obtained for CTQa_{CT}, CTQb_{CT} and CTQc_{CT} in aqueous solution simulated by the polarizable continuum model (PCM) model

Conformer	τ angle	Energy (kcal mol^{-1})	ΔE [a] (kcal mol^{-1})	ΔE [b] (kcal mol^{-1})	ΔE [c] (kcal mol^{-1})	Relative population[d]
CTQ$a1_{CT}$	76.72	−647,039.508	13.54	0.07	0.00	30.22
CTQ$a2_{CT}$	258.64	−647,039.160	13.67	0.42	0.35	16.78
CTQ$b1_{CT}$	77.20	−647,039.202	13.53	0.37	0.37	18.04
CTQb2_{CT}	258.01	−647,039.575	13.54	0.00	0.00	33.85
CTQ$c1_{CT}$	76.35	−647,037.299	15.51	2.28	0.00	0.72
CTQc2_{CT}	258.81	−647,036.932	15.53	2.64	0.37	0.39

[a] Solution-vacuum energy difference

[b] Energy difference relative to the most stable conformer

[c] Energy difference relative to the most stable conformer in each group

[d] Percent relative population calculated by Boltzmann, expressed in %

critical points [BCP, CP (3, −1)] constitute a powerful tool to classify a given chemical structure.

Negative eigenvalues of the Hessian matrix (λ_1 and λ_2, respectively) measure the degree of contraction of ρ in the normal direction of the bond to the PC, while a positive eigenvalue (e.g., λ_3) gives a quantitative indication of the degree of contraction parallel to the bond, and from the PC to each of the neighboring nuclei.

When the positive eigenvalue is dominant, the electron density is concentrated locally at each atomic basin. The interaction is classified as a closed shell and is typical in ionic bonds, hydrogen bonds, and van der Waals interactions. This interaction is described by relatively low values of ρ_b, $\nabla^2\rho_b > 0$ and $|\lambda 1|/\lambda 3 < 1$ and $G_b > 1$.

As supplementary material, the values of the electron charge density (ρ_b), Laplacian of the charge density ($\nabla^2\rho_b$), eigenvalues of the Hessian matrix (λ_1, λ_2 and λ_3), ellipticity (ε), kinetic energy density (G_b), and $|\lambda_1|/\lambda_3$ and G_b/ρ_b relationships are shown in the BCP for all chemical bonds expected for the lowest energy Z1-type conformers of CTQ*a1* and CTQ*b1* both in gas phase, and simulating the presence of an aqueous solvent. Variations of these parameters in solution were expressed as percentage differences calculated from:

$$\%\Delta x = \frac{x(solution) - x(vacuum)}{x(vacuum)} \times 100$$

Table 3 Energy calculated at B3LYP/6-31G(d,p) level of theory corrected by ZPE for the different possible conformations of resorcinol ring in gas and aqueous phase of CTQ*a*. Values are expressed in kcal mol^{-1}

Conformer	ΔE_{vacuum}[a]	$\Delta E_{solution}$[a]
Energy[b]	−647025.969	−647039.575
CTQa_{CT}	0.00	0.00
CTQa_{CC}	0.75	0.12
CTQa_{TC}	1.21	0.99
CTQa_{TT}	1.28	0.98

[a] Energy difference respect to the most stable conformer

[b] Energy of the most stable conformer at the B3LYP/6-31G(d,p) level of theory corrected by zero point energy (ZPE)

Through the analysis of the BCP, all C–C and C–H bonds of rings A and B of the analyzed conformers were characterized by a high value of ρ_b, $\nabla^2\rho_b < 0$, $|\lambda_1|/\lambda_3 > 1$ and $G_b/\rho_b < 1$, meaning that the negative curvature predominated, and the electronic charge was concentrated locally in the interatomic region, leading to the characterization of a typically polar covalent interaction.

As the C8a–O1 bond showed a high value of ρ_b and $\nabla^2\rho_b < 0$, but $|\lambda_1|/\lambda_3 < 1$ and $G_b/\rho_b > 1$, it was classified as an intermediate polar covalent interaction. This classification was due to an increased positive eigenvalue of the Hessian matrix. This behavior is typical of C–O bonds in pyran rings, where the C atom is also sp^2 hybridized, as reported for (4α→6″,2α→O→1″)-phenylflavan substituted with R = OH [18].

The characteristics of the interactions described so far were not affected significantly by the inclusion of solvent effect, but changes were found in critical points (3, −3) or nuclear critical points (NCP) in solution. Regarding the aromatic hydrogen atoms, there was a decrease in electron density in NCP, which did not exceed 1 %. However, the NCP values of the hydrogen atoms of the hydroxyls decreased by up to 4 % with respect to those in gas phase.

These changes were remarkable in relation to the characteristics of the MEP, as discussed below (Fig. 5). Interestingly, the values of the NCP electron density of the aromatic hydrogen of (4α→6″,2α→O→1″)-phenylflavan substituted with R = OH decreased in the range 0.7–1.2 %, while for the hydrogens of the OH groups the value decreased by up to 7.3 % [19]. At this point, we emphasize the lower density decrease in CTQ NCPs,

and relate this behavior with the lower stabilization of CTQ in solution than that reported for (4α→6″,2α→O→1″)-phenylflavan substituted with R = OH [18].

Another parameter of interest is the ellipticity (ε), defined as $\lambda_1/\lambda_2 - 1$, where λ_1 and λ_2 are the two negative curvatures of a BCP. In a bond with cylindrical symmetry, these two curvatures are of equal magnitude, and ellipticity is zero. However, when the electronic charge is accumulated in a given plane, along the bond path (for example, in a π bond), the decrease rate of ρ along the axis that lies in this plane is smaller than along an axis perpendicular to it, and the magnitude of the corresponding curvature of ρ is smaller. In this case ellipticity is greater than zero.

Topological properties at BCP in CTQ$a1_{CT}$ conformers and CTQ$b1_{CT}$ conformers in vacuum and in aqueous solution are given in Tables S3a and S3b.

Both in gas phase and in solution, the average value of ellipticity (ε) was greater in ring A than in ring B, as reported for (4α→6″,2α→O→1″)-phenylflavan substituted with R = OH.

In aqueous solution, the ellipticity of ring B decreased up to 4.5 %, (ellipticity of ring A up to 2.5 %). This also indicated a greater solvent effect on ring B in CTQ. In (4α→6″,2α→O→1″)-phenylflavan substituted with R = OH a similar behavior was found, but the ellipticity decrease in ring A was more marked (up to 5.3 %) . The minor decrease in ellipticity of resorcinol ring bonds shown in CTQ with respect to the values reported for (4α→6″,2α→O→1″)-phenylflavan substituted with R = OH, was also proposed as an interesting marker of lower stabilization in solution.

NBO analysis

Molecular orbital theory can report successfully on various properties of chemical systems using delocalized molecular orbitals, and requires approaches including electron correlation as well as a large enough basis set. Indeed, NBO analysis [29] is a technique for obtaining localized orbitals from ab initio wave functions. These orbitals can be identified with bonds, lone pairs, and antibonds. In simple terms, the delocalized molecular orbitals comprising an ab initio wave function are converted into NBOs through a series of matrix transformations. Transforming the ab initio wave functions into localized natural orbitals defines representations that are in good agreement with the concepts of Lewis chemical structure. Moreover, the overall transformation to NBOs also leads to unoccupied orbitals in the Lewis formal structure that can be used in the description of non-covalent effects.

For each donor NBO (*i*) and acceptor NBO (*j*), the second order stabilization energy ($E^{(2)}$) associated with *i/j* delocalization was estimated using the following expression:

$$E^{(2)} = -n_i \frac{F_{ij}^2}{\varepsilon_j - \varepsilon_i}$$

where n_i is the occupation or population of the donor orbital *i*; ε_i and ε_j are the energies of the orbitals involved in the interaction, and $F_{i,j}$ is the element *i,j* of the Fock matrix.

NBO analysis thus allowed us to investigate the main hyperconjugative interactions involved in the stability of the different conformers studied. The sum of the second order stabilization energies $E^{(2)}$, which described the charge delocalization effects, and explained the greater stability of Z1 compared to Z2 rotamers, is shown in Table 4.

In this table, the important role of electronic charge transfers to and from the ring C bonds in stabilizing both rotamers, as well as LP transfers from O3 and O atoms of this ring, was observed. These results demonstrated, as in (4α→6″,2α→O→1″)-phenylflavan substituted with R = OH [19], that, in spite of being a non-planar structure, ring B was not independent of ring A, and there were specific mechanisms of charge delocalization that defined interactions between rings A, C, and B.

Because of the greater stability of Z1 compared to Z2 rotamers, we selected the four structures of Z1-type rotamers belonging to groups CTQ*a* and CTQ*b* for further analysis.

NBO analysis allowed us to describe charge delocalizations explaining the energy ordering shown in Table 1 (CTQ$a1_{CT}$ > CTQ$b1_{CT}$ > CTQ$b2_{CT}$ > CTQ$a2_{CT}$, in order of decreasing stability), as indicated in Table 5.

These transfers account for charge delocalizations occurring in ring B, thus indicating the relevance of this region for stabilizing the system. However, looking at compound CTQ*b2*, the sum values of these transfers did not follow the trend. According to Table 5, the highest delocalization in ring B was reported for this structure; however, it was not stable. These results could be explained by observing that the substituent at 5-position of CTQ*b2* was located away from the plane defined by ring A (see H5–O5–C5–C6 dihedral angle in Table 5), thus decreasing all charge delocalization associated with that group. Therefore, our results indicated that, in CTQ*b2*, there was a destabilizing structural factor in another region of the system, which counteracted the greater delocalization found in the region of ring B, and explained the energetic stabilization order, CTQ*a1* > CTQ*b1* > CTQ*b2* > CTQ*a2*.

It is also interesting to note that the predominant resonance structure for CTQ*b1* was different from those obtained for the other conformers, as indicated by NBO analysis (see Figure S4 in Supplementary Material).

The modification introduced by the solvent in the CTQ conformational space led to the following order of decreasing

Table 4 Second order energies associated with charge transfers that account for the increased stability of Z1 against Z2 rotamers in gas phase, calculated at the B3LYP/6-311++G(d,p) level of theory. Values are expressed in kcal mol^{-1}

		CTQ*a*				CTQ*b*			
		Z1		Z2		Z1		Z2	
Donor	Acceptor	CTQ*a1*	CTQ*a2*	CTQ*a3*	CTQ*a4*	CTQ*b1*	CTQ*b2*	CTQ*b3*	CTQ*b4*
$\sigma_{O\text{-}C2}$	$\sigma^*_{C1'\text{-}C2'}$	1.87	2.04	1.60	1.46	1.87	1.88	1.20	1.42
$\sigma_{C2\text{-}C1'}$	$\sigma^*_{C8a\text{-}O}$	2.43	2.47	2.44	2.43	2.44	2.45	2.43	2.44
	$\sigma^*_{C2\text{-}C3}$	0.67	0.65	0.60	0.61	0.66	0.67	0.63	0.60
	$\sigma^*_{C3\text{-}C4}$	1.51	1.54	1.25	1.26	1.52	1.53	1.27	1.26
	$\sum$	4.61	4.66	4.29	4.30	4.62	4.65	4.33	4.30
$1n_{O3}$		5.27	4.60	5.11	4.61	5.23	5.17	5.17	5.20
$2n_{O3}$		14.15	14.33	13.69	13.55	14.10	13.95	13.88	13.69
	$\sum$	19.43	18.83	18.80	18.16	19.33	19.12	19.05	18.89
$1n_{O}$	$\sigma^*_{C8a\text{-}C8}$		0.51						
	$\sigma^*_{C8a\text{-}C4a}$	6.87	6.94	6.73	6.73	6.90	6.91	6.74	6.72
	$\sigma^*_{C2\text{-}C3}$	2.01	2.14	1.78	1.74	2.02	2.08	1.77	1.77
	$\sum$	8.88	9.08	8.51	8.47	8.92	8.99	8.51	8.49
$1n_{O}$	$\sigma^*_{C2\text{-}C1'}$	0.98	1.02	0.93	0.91	0.99	0.99	0.86	0.91
	$\sum_{TOTAL}$	35.77	35.63	34.13	33.30	35.73	35.63	33.95	34.01

stability: CTQ*b2* > CTQ*a1* > CTQ*b1* > CTQ*a2* according to Table 2. The second order energies $E^{(2)}$ associated with the charge transfers that explained this ordering are shown in Table 6. Again, we observed the important role of charge delocalizations occurring in ring B. Moreover, the substituent at 5-position was no longer a destabilizing factor, since in solution the OH group approached the plane of ring A (see H5–O5–C5–C6 dihedral angle in Table 6).

Molecular electrostatic potential

MEP values have been used widely to predict the behavior and reactivity of a variety of chemical systems [34–38]. As other physicochemical parameters used as indicators of reactivity, the electrostatic potential V(r) is a physical property that can be determined both experimentally and by computational methods. The calculation of this physicochemical property on the molecular surface, and subsequent visualization by a color code, allows a different view of molecular behavior.

In this work, the procedure proposed by Politzer et al. [38] to predict sites susceptible to electrophilic attack in the region of negative values of V(r) was used. The most stable structures according to prior analysis in gas phase and in aqueous solution were studied. Our results showed that the sites more susceptible to electrophilic attack were located on oxygen atoms (Figs. 4, 5).

Comparing the maximum and minimum V(r) values in both media, the highest value (positive) showed an average increase of 37 % in solution, while the lowest (negative) value decreased by 21 % on average. These values showed a higher CTQ reactivity in aqueous solution (Table 7). These variations were lower than those observed for (4α→6″,2α→O→1″)-phenylflavan substituted with R = OH [19] [positive values increased by 46 %, while the negative V(r) values decreased 31 %].

It is interesting to note that the lower V(r) variation for CTQ [than for (4α→6″,2α→O→1″)-phenylflavan substituted with R = OH] in an aqueous medium with respect to values in vacuum, was consistent with its lower energy stabilization in aqueous solution.

The increase in the V(r) positive value on the hydroxyl hydrogen atoms of the catechol and resorcinol rings in solution

Table 5 Second order energies associated with charge transfers to explain the order of stability of Z1 conformers for CTQ*a* and CTQ*b*; calculated at the B3LYP/6-B3LYP/6-311++G(d,p) level of theory. Values are expressed in kcal mol^{-1}

Donor	Acceptor	CTQ*a1*	CTQ*b1*	CTQ*b2*	CTQ*a2*
$1n_{O3'/O4'}$	$\sigma^*_{O4'\text{–}H/O3'\text{–}H}$	0.98	0.96	0.98	0.97
$\sigma_{O4'\text{–}H/O3'\text{–}H}$	$\sigma^*_{C4'\text{–}C5'/C2'\text{–}C3'}$	5.51	5.55	5.58	5.51
$\sigma_{O3'\text{–}H/O4'\text{–}H}$	$\sigma^*_{C3'\text{–}C4'}$	3.94	3.89	3.90	3.90
$1n_{O4'/O3'}$	$\sigma^*_{C3'\text{–}C4'}$	6.28	6.27	6.26	6.27
	$\sum$	16.71	16.67	16.72	16.65
	H5–O5–C5–C6 dihedral angle	1.779	1.670	2.173	2.006

Table 6 Second order energies associated with charge transfers to explain the order of stability of Z1 conformers for CTQ*a* and CTQ*b*; calculated at the B3LYP/6-311++G(d,p) level of theory, considering the solvent effect by PCM model. Values are expressed in kcal mol^{-1}

Donor	Acceptor	CTQ*b2*	CTQ*a1*	CTQ*b1*	CTQ*a2*
$1n_{O3'/O4'}$	$\sigma^*_{O4'-H/O3'-H}$	1.04	1.03	1.01	1.02
$\sigma_{O4'-H/O3'-H}$	$\sigma^*_{C4'-C5'/C2'-C3'}$	5.61	5.52	5.55	5.51
$\sigma_{O3'-H/O4'-H}$	$\sigma^*_{C3'-C4'}$	4.10	4.13	4.10	4.11
$1n_{O4'/O3'}$	$\sigma^*_{C3'-C4'}$	6.26	6.26	6.25	6.26
	$\sum$	17.01	16.94	16.91	16.90
	H5–O5–C5–C6 dihedral angle	1.622	1.633	1.641	1.655

can be observed in Fig. 4. This modification can be rationalized based on the largest donor character of such O–H bonds with respect to gas phase, as shown in Table 8, and the major decrease in NCP density of the hydrogens of these bonds.

By comparing Tables 5 and 6, the effect of solvent on the charge transfers associated with the lone pairs of the O-3′ and O-4′ oxygen atoms was different. Indeed, in solution, the $1n_{O3',O4'} \rightarrow \sigma^*_{O-H}$ charge transfer was greater than that found in vacuum (increases), while the $1n_{O4',O3'} \rightarrow \sigma^*_{C3-C4}$ charge transfer decreased (increase of 5.4 %, and decrease of 0.2 % on average).

On the other hand, the charge transfers from the O-1 oxygen atom of ring C decreased in solution. In CTQ*a1*, for example, the decrease expressed as the percentage difference for $1,2n_{O1} \rightarrow \sigma^*, \pi^*$ transfers was −2.5 % [$\Delta_{Solvent-Vacuum}$ = (35.03–35.94) kcal mol^{-1}].

A greater surface corresponding to the negative potential on the oxygen atoms, whose donor role was lowered in solution, is shown in Fig. 5. This could indicate increased reactivity at these sites for electrophilic aromatic substitution reactions. In cases where the donor role increased, the opposite was observed. Therefore, the V(r) negative values can be interpreted from the donor role of the oxygen lone pairs.

Intramolecular hydrogen bond interactions in the catechol ring

The occurrence of hydrogen bonding (HB) in catechol rings has been widely reported [9, 27, 39].

In CTQ, at the level of calculation used, we found the following distances and angles: for CTQ*a*, O3′···H4′ 2.126 Å, O4′–H4′ 0.969 Å, lengthening of O4′–H4′ by 0.003 Å, O4′···O3′ 2.677 Å, and the angle O3′···H4′–O4′ = 114.53°; for CTQ*b*, O4′···H3′ 2.128 Å, O3′–H3′ 0.969 Å, lengthening of O3′–H3′ by 0.003 Å, O3′···O4′ 2.680 Å and the angle O4′···H3′–O3′ = 114.51°. Therefore, following these geometrical criteria, the existence of HB-type interactions can be characterized as weak hydrogen bonds (bond lengths A···H >> X–H, lengthening of X–H (Å) ≤0.01, distance (X···A) range (Å) = 3.0–4.0, distance (H···A) range (Å) = 2.0–3.0 and θ(X–H···A) range (°) = 90–180, where A designates the acceptor atom and X designates the donor atom [40]).

NBO analysis showed the existence of a $1n_O \rightarrow \sigma^*_{O-H}$ charge transfer between the lone pairs of the oxygen atom and the antibonding orbital of the hydroxyl, which is more effective in CTQ*a* than in CTQ*b*. Indeed, the values of the second order stabilization energy $E^{(2)}$ were 0.98 and 0.96 kcal mol^{-1}, respectively (Table 5), which were in agreement with the shortest distance for the first structure, and therefore, its greatest strength, and consequent major structural stabilization.

Even when using AIM analysis, it was not possible to confirm the existence of BCPs in the O···H region. Our results indicate, according to previous findings, the presence of HB-type interactions in ring B of CTQ*a* and CTQ*b*, confirming that the greater stability of the two conformers compared to

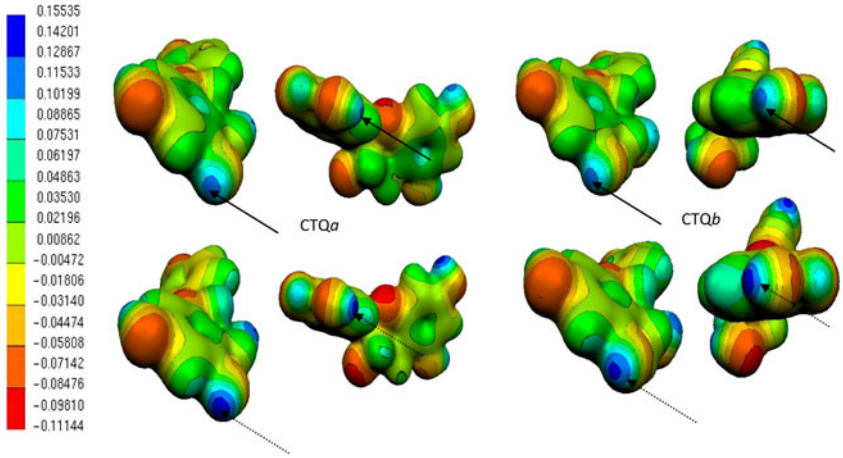

Fig. 4 Maps of molecular electrostatic potential (MEP) for minimum energy structures of the CTQ*a* and CTQ*b* groups, showing the change in the positive V(r) on the H atoms of hydroxyls. *Solid arrows* Behavior in vacuum, *dotted arrows* behavior in aqueous solution

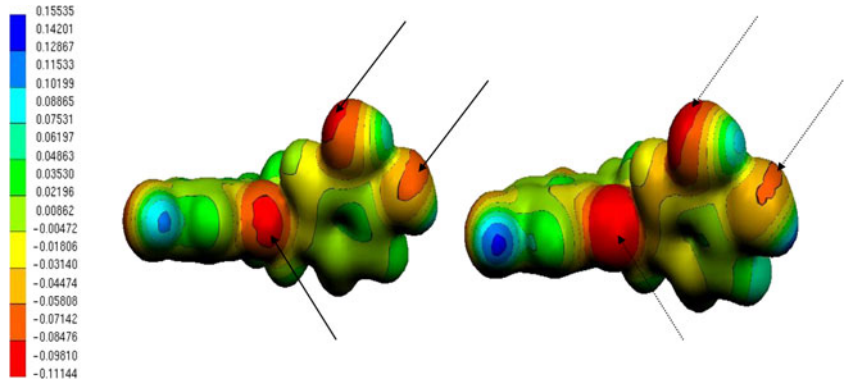

Fig. 5 MEP maps for the CTQ*b2* structure, showing the change in the V(r) negative value on the oxygen atoms due to the inclusion of the solvent effect. *Solid arrows* Values in vacuum, *dotted arrows* values in aqueous solution

CTQ*c* was due to the presence of intramolecular BH interactions in the catechol ring. The stabilizing effect of characterized HB-type interactions, estimated by calculating the energy difference between conformers belonging to CTQ*a* and CTQ*b* groups, and the structurally similar structure belonging to the CTQ*c* group is shown in Table 9.

The presence of solvent slightly affected HB-type interactions. The O···H distances did not vary appreciably (decreased by 0.01 % on average). The O···H–O angle decreased on average by 0.3 %. The $1n_O \rightarrow \sigma^*_{O\text{-}H}$ charge transfer increased on average by 5.4 % (Table 6). NBO analysis showed that this transfer was slightly more effective in CTQ*b* than in CTQ*a*, being second-order stabilization energy values $E^{(2)}$=1.04 and 1.03 kcal mol^{-1}, respectively.

By studying such interactions under the influence of an aqueous solvent, an energy difference of 2.25 kcal mol^{-1} was observed on average between the structures with a hydrogen bridge in the catechol ring (CTQ*a* and CTQ*b*), and those without one (CTQ*c*). The minor difference found in solution, despite the stronger HBs, was due to the fact that CTQ*c* structures showed an increased stabilization (about 2.0 kcal mol^{-1}) in the presence of the aqueous solvent (Table 2).

As already shown [18] for intramolecular C–O···H interactions, MEP analysis enabled us to identify easily and efficiently the presence of intramolecular HB type interactions; in this case for the structure of CTQ the presence of O···H–O intramolecular HB in the catechol ring. Indeed, the value of V(r) on the O atom involved in the HB bond (atom belonging to the hydrogen acceptor moiety) became less negative (greater) than the V(r) of the atom that was not involved in this interaction (e.g., $\Delta_{O3'\text{–}O4'}$ = ca. 17.0 kcal mol^{-1}). The positive V(r) value on the HB hydrogen atom of O···H (belonging to the hydrogen donor moiety) became more negative (lower) than on another hydrogen of the OH group (e.g., $\Delta_{H\neq4'\text{–}H4'}$ = ca. 33.0 kcal mol^{-1}). The V(r) value on the atom of the donor moiety decreased, while the V(r) value on the acceptor moiety increased. These variations were more pronounced in solution, which agreed with the greatest strength of the HB being found in aqueous medium (Fig. 6).

Table 7 Variation (Δ) of the maxima and minima V(r) electrostatic potential when considering the inclusion of the solvent effect by PCM model. Values are expressed in kcal mol^{-1}

	Vmax	Vmin
Vacuum	70.69	−57.66
Solution	97.48	−69.93
Δ (%)	37.91	21.28

Molecular polarizability

The values of molecular isotropic polarizability are important as indicators of the solubility and chemical reactivity of the molecules under study. Isotropic polarizability is a measure of electronic distortion in a molecule, caused by an external electric field, and is a good indicator of how the electric charge distribution of a molecule is affected [41].

In this paper, calculations of the polarizability $\langle\alpha\rangle$ (Table 10) for CTQ were performed according to the following expression:

$$\langle\alpha\rangle = \frac{1}{3}\left(\alpha_{xx} + \alpha_{yy} + \alpha_{zz}\right)$$

where tensor components were obtained from the second derivative of the energy with respect to the Cartesian components of the applied electric field ε, $\alpha=[\partial^2 E/\partial\varepsilon^2]$. To take into

Table 8 Second order energies associated with the charge transfers of the OH groups of the most stable structures in vacuum and in aqueous solution, calculated at the B3LYP/6-311++G(d,p) level of theory. Values are expressed in kcal mol^{-1}

Donor	CTQ*a1*			CTQ*b2*		
	Vacuum	Solution	Δ (%)	Vacuum	Solution	Δ (%)
O3′-H/O4′-H	3.94	4.13	4.82	3.90	4.10	5.13
O4′-H/O3′-H	5.51	5.52	0.18	5.58	5.61	0.54
O5-H	4.42	4.51	2.04	4.41	4.51	**2.27**
O7-H	5.15	5.16	0.19	5.15	5.16	0.19

Table 9 Energy difference (kcal mol^{-1}) in gas phase and in aqueous solution between conformers belonging to CTQ*a* and CTQ*b* groups with a similar arrangement of ring B, and the corresponding structures of the CTQ*c* group, in which there is no intramolecular HB

	Vacuum		Solution	
X	CTQ*a*	CTQ*b*	CTQ*a*	CTQ*b*
$\Delta_{CTQc1\text{-}X1}$	4.18	3.87	2.21	1.90
$\Delta_{CTQc3\text{-}X3}$	3.97	3.66		
$\Delta_{CTQc2\text{-}X2}$	4.09	4.23	2.23	2.64
$\Delta_{CTQc4\text{-}X4}$	4.30	3.86		
Average	4.13	3.90	2.22	2.27

account the weight of the 12 different conformers analyzed, the mean statistically value was calculated by Maxwell-Boltzmann distribution of the polarizability at 298.15 K, as the following expression:

$$\langle\alpha\rangle = \sum_i < \alpha_i > \exp\left(\frac{-Ei}{RT}\right) / \sum_i \exp\left(\frac{-Ei}{RT}\right)$$

This value was 175.88 a.u., indicating the soluble nature in polar solvents, and its ability to polarize other atoms and molecules. The value found for <α> in (4α→6″,2α→O→1″)-phenylflavan substituted with R = OH was 222.24 a.u. [19]. It is interesting to note the increased polarizability of CTQ*c* conformers, which explained their greater stabilization in solution.

These results led to the observation that the lower CTQ stabilization in aqueous solution could be explained by a lower <α> value.

Conclusions

This study of the conformational space of catechin analyzed and characterized in vacuum 12 CT-type conformers, which were classified into three defined groups by the arrangement of the OH groups of ring B ($CTQa1_{CT}$ > $CTQb1_{CT}$ > $CTQb2_{CT}$ > $CTQa2_{CT}$ > $CTQc1_{CT}$ > $CTQc2_{CT}$, accounting for decreasing stability). Moreover, for each group, two types of structure (Z1 and Z2) were further characterized according to ring B arrangement. Including long range effect of aqueous solvent by the PCM model, the conformational space was modified ($CTQb2_{CT}$ > $CTQa1_{CT}$ > $CTQb1_{CT}$ > $CTQa2_{CT}$ > $CTQc1_{CT}$ > $CTQc2_{CT}$, in decreasing stability order), and the set reduced to only six Z1-type conformers.

We concluded that long-range solvent effects lead to a lengthening of all bonds except C–O bonds and that OH substituents are arranged closer to the plane of the rings to which they were attached. Moreover, solvent affected mostly the position of ring B relative to the A-C system, and modified the position of the OH groups of that ring, without influencing the resorcinol-type ring. The solvent also attenuated the energy difference between conformers.

Table 10 Polarizability values for all CTQ conformers calculated at the B3LYP/6-31G(d,p) level of theory in gas phase[a]

Conformer	α_{xx}	α_{yy}	α_{zz}	<α>
CTQ*a1*	250.14	170.00	107.39	175.84
CTQ*a3*	247.26	187.14	91.31	175.24
CTQ*a2*	256.19	171.52	100.36	176.02
CTQ*a4*	250.95	181.55	93.71	175.41
CTQ*b1*	256.60	166.56	104.88	176.01
CTQ*b3*	250.77	176.75	99.00	175.51
CTQ*b2*	252.59	170.03	105.18	175.93
CTQ*b4*	249.23	182.16	94.65	175.35
CTQ*c1*	252.08	170.64	106.72	176.48
CTQ*c3*	248.62	186.33	92.63	175.86
CTQ*c2*	254.90	172.90	101.93	176.57
CTQ*c4*	251.24	189.91	86.62	175.92

[a] All values are expressed in a.u.

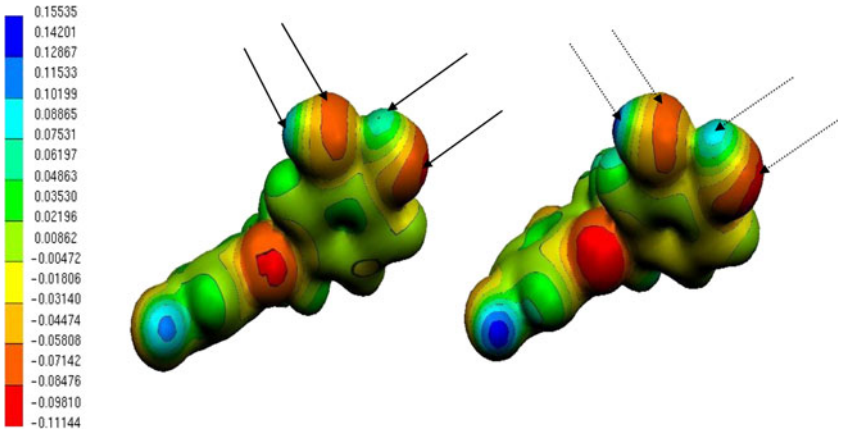

Fig. 6 MEP maps for the CTQ*a1* structure, showing the change in the positive V(r) value on H atoms, and O of hydroxyls whether involved in an intramolecular hydrogen bridge (HB) or not. *Solid arrows* Values in vacuum, *dotted arrows* values in aqueous solution

We characterized all bonding interactions and concluded that the BCP topological parameters were not affected significantly by the inclusion of the solvent effect, but changes were observed in critical points (3, −3) or NCPs and in ellipticity (ε) values. A major decrease of ε was found in ring B, thus indicating a greater long-range effect of solvent on ring B of CTQ.

Despite being a non-planar structure, it was concluded that the charge delocalizations in CQT occurring in ring B indicate that it is not independent of ring A, thus highlighting the importance of this region of the system for stabilization thereof.

Sites more susceptible to electrophilic attack were located on the oxygen atoms, and the higher reactivity of CTQ in aqueous solution was also demonstrated. It was concluded that the changes in donor character of the O–H bonds, the NCP density of their hydrogen atoms and the donor role of the lone pairs of the oxygen atoms, correlated with changes in the positive V(r) values on hydrogens of the hydroxyls belonging to catechol and resorcinol rings and in the negative V(r) values on oxygen atoms in solution.

Intramolecular HB interactions in the catechol moiety, at the level of calculation, can be characterized by geometric criteria, NBO analysis, and MEP study. The presence of solvent affected the interactions slightly, increasing their strength.

We concluded that the polarizability of CQT was lower than that obtained for (4α→6″,2α→O→1″)-phenylflavan substituted with R = OH, and this explained the lower stabilization of CTQ in solution. Furthermore, we concluded that this lower stabilization of CTQ in solution with respect to (4α→6″,2α→O→1″)-phenylflavan substituted with R = OH was associated with the following long range solvent effects:

- Minor lengthening of C–C, C–H, and O–H bonds.
- Less shortening of C–O bonds.
- Minor decrease in NCP electron density of hydrogen atoms.
- Minor decrease in bond ellipticity of resorcinol-type rings.
- Less variation in MEPs.

Work considering explicit solvation effects is in progress.

Acknowledgments Thanks are due to the National Council of Scientific and Technical Researches of Argentina (CONICET) and Universidad de Buenos Aires (Argentina) for financial support. A.B..P. is a Senior Research Member of the National Research Council of Argentina (CONICET). E.N.B. acknowledges a fellowship from the National Council of Scientific and Technical Researches of Argentina (CONICET) and Universidad de la Cuenca del Plata (Corrientes, Argentina). R.M.L. acknowledges Universidad de la Cuenca del Plata and Universidad Nacional del Nordeste and Centro de Cómputos de Alto Desempeño de la Universidad Nacional del Nordeste (CADUNNE) for facilities provided during the course of this work.

References

1. Visioli F, Bellomo G, Galli C (1998) Free radical-scavenging properties of olive oil polyphenols. Biochem Biophys Res Commun 247: 60–64
2. Visioli F, Galli C (1998) Olive oil phenols and their potential effects on human health. J Agric Food Chem 46:4292–4296
3. Mercader AG, Pomilio AB (2012) (Iso)Flav(an)ones, chalcones, catechins, and theaflavins as anticarcinogens: mechanisms, anti-multidrug resistance and QSAR studies. Curr Med Chem 19:4324–4347
4. Mercader AG, Pomilio AB (2011) Biflavonoids: occurrence, structural features and bioactivity. Nova Science, New York, 978-1-62100-354-0
5. Mercader AG, Pomilio AB (2013) Naturally-occurring dimers of flavonoids as anticarcinogens. Anticancer Agents Med Chem 13(8): 1217–1235
6. Harborne JB, Williams CA (2000) Advances in flavonoid research since 1992. Phytochemistry 55:481–504
7. Elhabiri M, Figueiredo P, Toki K, Saito N, Brouillard RA (1997) Anthocyanin–aluminium and –gallium complexes in aqueous solution. J Chem Soc Perkin Trans 2:355–362
8. Pérez-González A, Rebollar-Zepeda AM, León-Carmona JR, Galano A (2012) Reactivity indexes and O–H bond dissociation energies of a large series of polyphenols: implications for their free radical scavenging activity. J Mex Chem Soc 56(3):241–249
9. Mendoza-Wilson AM, Lardizabal-Gutiérrez D, Torres-Moye E, Fuentes-Cobas L, Balandrán-Quintana RR, Camacho-Dávila A, Quintero-Ramos A, Glossman-Mitnik D (2007) Optimized structure and thermochemical properties of flavonoids determined by the CHIH(medium) DFT model chemistry versus experimental techniques. J Mol Struct 871:114–130
10. Mendoza-Wilson AM, Glossman-Mitnik D (2006) Theoretical study of the molecular properties and chemical reactivity of (+)-catechin and (−)-epicatechin related to their antioxidant ability. J Mol Struct THEOCHEM 761:97–106
11. Zhang J, Du F, Peng B, Lu R, Gao H, Zhou Z (2010) Structure, electronic properties, and radical scavenging mechanisms of daidzein, genistein, formononetin, and biochanin A: a density functional study. J Mol Struct THEOCHEM 955:1–6
12. Markovic ZS, Mentus SV, Dimitric Markovic JM (2009) Electrochemical and density functional theory study on the reactivity of fisetin and its radicals: implications on in vitro antioxidant activity. J Phys Chem A 113:14170–14179
13. Rice-Evans CA, Miller NJ, Paganga G (1996) Structure-antioxidant activity relationships of flavonoids and phenolic acids. Free Radical Biol Med 7:933, and references therein
14. Zhang HY, Wang LF, Sun YM (2003) Why B-ring is the active center for genistein to scavenge peroxyl radical: a DFT study. Bioorg Med Chem Lett 13:909–911
15. Antonczak S (2008) Electronic description of four flavonoids revisited by DFT method. J Mol Struct THEOCHEM 856:38–45
16. Leopoldini M, Russo N, Toscano M (2007) A comparative study of the antioxidant power of flavonoid catechin and its planar analogue. J Agric Food Chem 55:7944–7949
17. Lobayan RM, Jubert AH, Vitale MG, Pomilio AB (2009) Conformational and electronic (AIM/NBO) study of unsubstituted A-type dimeric proanthocyanidin. J Mol Model 15:537–550
18. Bentz EN, Jubert AH, Pomilio AB, Lobayan RM (2010) Theoretical study of Z isomers of A-type dimeric proanthocyanidins substituted with R = H, OH and OCH_3: stability and reactivity properties. J Mol Model 16:1895–1909
19. Lobayan RM, Bentz EN, Jubert AH, Pomilio AB (2012) Structural and electronic properties of Z isomers of (4α → 6",2α → O → 1")-phenylflavans substituted with R = H, OH and OCH3 calculated in

aqueous solution with PCM solvation model. J Mol Model 18:1667–1676
20. Lobayan RM, Bentz EN, Jubert AH, Pomilio AB (2013) Charge delocalization in Z- isomers of (4α → 6",2α → O → 1")-phenylflavans with R = H, OH and OCH3. Effects on bond dissociation enthalpies and ionization potentials. J Comput Theor Chemistry 1006:37–46
21. Olejniczak S, Potrzebowski MJ (2004) Solid state NMR studies and density functional theory (DFT) calculations of conformers of quercetin. Org Biomol Chem 2:2315–2322
22. Miertus S, Scrocco E, Tomasi J (1981) Electrostatic interaction of a solute with a continuum. A direct utilizaion of ab initio molecular potentials for the prevision of solvent effects. J Chem Phys 55:117–129
23. Frisch MJ, Trucks GW, Schlegel HB, Scuseria GE, Robb MA, Cheeseman JR, Montgomery JA, Vreven T Jr, Kudin KN, Burant JC, Millam JM, Iyengar SS, Tomasi J, Barone V, Mennucci B, Cossi M, Scalmani G, Rega N, Petersson GA, Nakatsuji H, Hada M, Ehara M, Toyota K, Fukuda R, Hasegawa J, Ishida M, Nakajima T, Honda Y, Kitao O, Nakai H, Klene M, Li X, Knox JE, Hratchian HP, Cross JB, Adamo C, Jaramillo J, Gomperts R, Stratmann RE, Yazyev O, Austin AJ, Cammi R, Pomelli C, Ochterski JW, Ayala PY, Morokuma K, Voth GA, Salvador P, Dannenberg JJ, Zakrzewski VG, Dapprich S, Daniels AD, Strain MC, Farkas O, Malick DK, Rabuck AD, Raghavachari K, Foresman JB, Ortiz JV, Cui Q, Baboul AG, Clifford S, Cioslowski J, Stefanov BB, Liu G, Liashenko A, Piskorz P, Komaromi I, Martin RL, Fox DJ, Keith T, Al-Laham MA, Peng CY, Nanayakkara A, Challacombe M, Gill PMW, Johnson B, Chen W, Wong MW, Gonzalez C, Pople JA (2003) Gaussian 03, revision B.02. Gaussian, Pittsburgh
24. Lee C, Yang W, Parr RG (1988) Development of the Colle-Salvetti correlation-energy formula into a functional of the electron density. Phys Rev B 37:785–789
25. Becke AD (1993) Density-functional thermochemistry. III. The role of exact exchange. J Chem Phys 98:5648–5652
26. Leopoldini M, Marino T, Russo N, Toscano M (2004) Antioxidant properties of phenolic compounds: H-atom *versus* electron transfer mechanism. J Phys Chem A 108:4916–4922
27. Zhang HY, Sun YM, Wang XL (2003) Substituent effects on O–H bond dissociation enthalpies and ionization potentials of catechols: a dft study and its implications in the rational design of phenolic antioxidants and elucidation of structure–activity relationships for flavonoid antioxidants. Chem-A Eur J 9:502–508
28. Bader RFW (1995) Atoms in molecules—a quantum theory. Oxford University Press, Oxford
29. Glendening ED, Reed AE, Carpenter JE, Weinhold F NBO 3.1. Program as implemented in the Gaussian 98 package. Gaussian, Wallingford, CT
30. Biegler-Koning FW, Bader RFW, Tang TH (1982) Calculation of the average properties of atoms in molecules II. J Comput Chem 3:317–328
31. Flúkiger P, Lúthi HP, Portmann S, Weber J (2000) MOLEKEL 4.0. Swiss Center for Scientific Computing, Manno
32. Bader RFW (1990) A quantum theory of molecular structure and its applications. Chem Rev 91:893–928
33. Bader RFW (1998) A bond path: a universal indicator of bonded interactions. J Phys Chem A 102:7314–7323
34. Politzer P, Landry SJ, Warnheim T (1982) Proposed procedure for using electrostatic potentials to predict and interpret nucleophilic processes. J Phys Chem 86:4767–4771
35. Politzer P, Abrahmsen L, Sjoberg P (1984) Effects of amino and nitro substituents upon the electrostatic potential of an aromatic ring. J Am Chem Soc 106:855–860
36. Politzer P, Laurence PR, Jayasuriya K (1985) Molecular electrostatic potentials: an effective tool for the elucidation of biochemical phenomena. Environ Health Perspect 61:191–202
37. Roy DK, Balanarayan P, Gadre SR (2009) Signatures of molecular recognition from the topography of electrostatic potential, J. Chem Sci 121:815–821
38. Politzer P, Truhlar DG (eds) (1981) Chemical applications of atomic and molecular electrostatic potentials. Plenum, New York
39. Aparicio S (2010) A systematic computacional study on flavonoids. Int J Mol Sci 11:2017–2038
40. Desiraju GR, Steiner T (1999) The weak hydrogen bond in structural chemistry and biology. Oxford University Press, New York
41. Weber KC, Honório KM, Bruni AT, da Silva ABF (2006) The use of classification methods for modeling the antioxidant activity of flavonoid compounds. J Mol Model 12:915–920